University Library

A gateway to Melbourne's research publications

Minerva Access is the Institutional Repository of The University of Melbourne

Author/s:
Yuan, G;Gómez, D;Kirkwood, N;Mulvaney, P

Title:
Tuning Single Quantum Dot Emission with a Micromirror

Date:
2018-02-14

Citation:
Yuan, G., Gómez, D., Kirkwood, N. & Mulvaney, P. (2018). Tuning Single Quantum Dot Emission with a Micromirror. Nano Letters, 18 (2), pp.1010-1017. https://doi.org/10.1021/acs.nanolett.7b04482.

Persistent Link:
https://hdl.handle.net/11343/344947

Tuning Single Quantum Dot Emission with a Micro-mirror

Gangcheng Yuan[1], Daniel Gómez[2], Nicholas Kirkwood[1], Paul Mulvaney[1]*

Email: mulvaney@unimelb.edu.au

ph: +61 3 8344 2405

1 ARC Centre of Excellence in Exciton Science, School of Chemistry, University of Melbourne, Parkville, Victoria, 3010, Australia

2 School of Chemical Sciences, RMIT University, Melbourne, Victoria, 3001, Australia

ABSTRACT: The photoluminescence of single quantum dots fluctuates between bright (*on*) and dark (*off*) states, also termed fluorescence intermittency or blinking. This blinking limits the performance of quantum dot based devices such as light-emitting diodes and solar cells. However, the origins of the blinking remain unresolved. Here, we use a movable gold micro-mirror to determine both the quantum yield of the bright state and the orientation of the excited state dipole of single quantum dots. We observe that the quantum yield of the bright state is close to unity for these single QDs. Furthermore, we also study the effect of a micro-mirror on blinking, and then evaluate excitation efficiency, biexciton quantum yield, and detection efficiency. The mirror does not modify the

off-time statistics, but it does change the density of optical states available to the quantum dot and hence the *on* times. The duration of the *on* times can be lengthened due to an increase in the radiative recombination rate.

KEYWORDS Quantum dot, blinking, CdSe, quantum yield, ionization

The emission quantum yield (QY) is one of the basic but important properties of fluorophores such as quantum dots (QDs). Ultimately, the QY defines the upper efficiency limit of devices such as light-emitting diodes. The photoluminescence (PL) QY is the ratio of the number of photons emitted to the number of photons absorbed by an emitter. It is directly related to the exciton dynamics in QDs, especially the competition between the radiative and non-radiative decay pathways. The relative PL QY can be measured in dilute solution by comparing the emission intensity of QD ensembles to that of a standard system with the same absorption.[1-3] While relative QY measurements are convenient, the accuracy of the QY measurement depends on the standards used. A standard-free QY measurement can be realized *via* the Purcell effect,[4] *i.e.,* by recognizing that the spontaneous radiative decay rate is not an intrinsic property but is environment-dependent. Drexhage[5] was the first to investigate this effect. He actively modified the fluorescence lifetime of ensembles of Eu^{3+} ions using a planar dielectric and metal structure. Variations in the radiative fluorescence lifetime could be accounted for quantitatively by considering the change in the local density of optical states (LDOS), using either a classical or quantum model to describe the planar structures.[6-8] The intrinsic non-radiative decay rate is not modified by the LDOS; hence, we can measure the absolute QY from the variations in the measured total fluorescence lifetime when the optical environment is changed. Similar methods have been applied to several kinds of ensemble emitters such as ions,[9] molecules,[10-12] and QDs,[13-15] but they can also be used to measure the QY of single emitters if they are photostable enough.[16-19] The real experimental challenge is due to the fact that the PL from single QDs exhibit blinking or fluorescence intermittency.

It has been over twenty years since the first observation of fluorescence intermittency in single QDs.[20] The emission from a single QD randomly switches between the *on* and *off* states, a process attributed to charging and discharging of the QD.[21] During the *on* periods, the PL QY is high because the QD is in a neutral state. During the *off* periods, the QD is ionized, and then non-radiative Auger recombination quenches the emission. In addition to these two states, it has been reported that there exists a continuous distribution of emission states with different QYs.[22] This has led to a second blinking model based on multiple recombination centers without invoking charging and discharging.[23] Irrespective of the model which determines blinking, the QYs of grey states are lower than 1.

If the QY of the bright state is 1, the QYs of grey states should be related to the emission intensity ratios of the grey states to the bright state.[24] Therefore, it is important to know whether the QY of the bright state or *on* state is 1. Several groups have studied this aspect. Broxmann et al.[25] modified the fluorescence of single QDs and measured the single QD QYs by confining the QD using dielectric interfaces. Burchler et al.[17] placed a movable silver mirror near a single terrylene molecule and were able to extract its QY. By continuously changing the LDOS *via* the mirror position, the PL lifetime was observed to continuously vary.[16-19] From this variation, the QY can be obtained. This method can also be used to evaluate the QYs of single QDs, in particular due to their superior photostability. However, a complication in these measurements is the multi-state nature of QD blinking.

It is widely known that blinking is sensitive to the chemical or electrical environment of the nanocrystal because the trapping process is modified.[26] Blinking can also be changed (supp

ressed) by plasmonic coupling between QDs and a thin gold film.[27-29] Similar effects have also been reported for QDs coupled to optical antennas.[30-35] The coupling enhances significantly the total decay rate k_{total} by increasing the energy transfer rate k_{metal}, and hence the Auger decay rate k_A can become negligible ($k_{total} = k_{metal} + k_A \approx k_{metal}$). Then the QYs of both the neutral and charged states become equal, QY $= k_{rad}/k_{metal}$. Therefore, even though the QDs are still undergoing charging and discharging, there is little or no fluctuation in the PL intensity. In addition to this conventional explanation, blinking suppression may be realized by reducing the ionization rate.[30] In principle, if there is sufficient enhancement of the radiative rate *via* changes in the LDOS, the exciton lifetime can be decreased so much that there is an extremely low probability of exciton ionization.

In this paper, we have used Drexhage's method to measure the QY and orientation of single QDs with a movable micro-mirror. The PL QY of the bright state is close to 1 for our single QDs. We have studied the blinking behavior of a single QD close to and far away from the mirror. We find that although the power-law distributions of *on*- and *off*-times are not changed, the ionization process can be suppressed either by reducing the excitation rate or by increasing the exciton relaxation rate.

Figure 1a shows a schematic of the combination of JPK AFM and a home-made confocal microscope. The graded shell CdSe/$Cd_xZn_{1-x}S$ QDs used here are very photostable due to high-temperature annealing and smooth core-shell barriers.[36] In order to fix the QD position and orientation during measurements, the QDs were embedded in a 10 nm-thick PMMA film on glass. The laser was focused onto a single QD through an objective mounted on a piezo stage. In order to avoid photodamaging the QDs, the laser power was reduced to the lowest practical level. To fabricate a micro-mirror, a gold-coated microsphere was glued onto an AFM cantilever (see scanning electron microscopy image (SEM) in Figure 1b). The mirror mounted on the AFM scanned across the surface of dilute QD films in contact mode or tapping mode. We constructed a map of the intensity of the laser light reflected by the mirror (Figure 1c), which resembles Newton's rings. By positioning the microsphere in the center of the rings and quenching the maximum of the emission from a single QD, the laser spot, the QD and the apex of the microsphere could be accurately aligned. After alignment, the emission of the QD was measured whilst varying the distance d between the mirror and the glass surface as shown in Figure 1d.

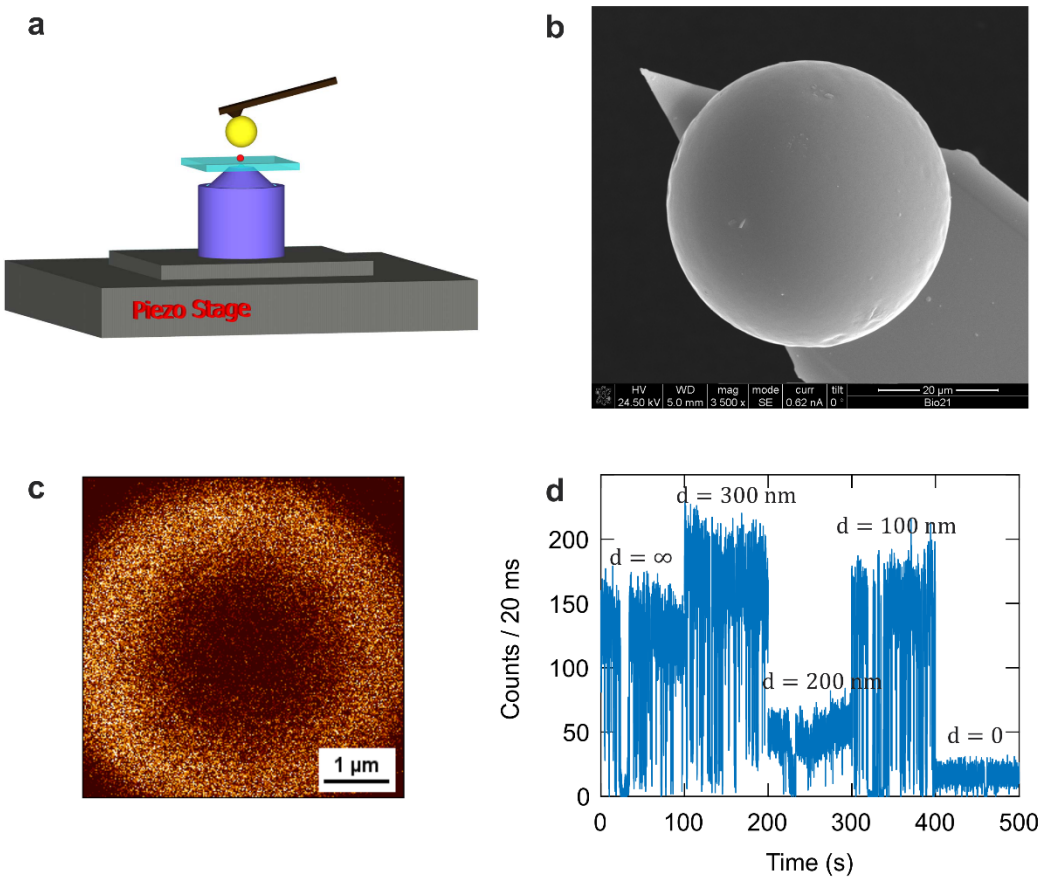

Figure 1 **(a)** Schematic of the AFM-confocal-microscope set-up. **(b)** SEM image of a gold-coated microsphere (49 μm diameter) attached to a cantilever. The gold surface of the microsphere can be approximated as a plane mirror at small separations. **(c)** A typical laser reflection map. When the tip is scanning across the surface, the reflected light from the micro-mirror is collected by the objective. **(d)** PL intensity trace from a single QD as a function of the distance between the mirror and the sample.

QY and Orientation Measurement

Figure 2 shows how the PL lifetime varies in response to the changing distance between the micro-mirror and the QDs. In principle, we can analyze the lifetime variation and then obtain the QY for every emission state. In practice, however, we only analyzed variations

in the PL lifetime of the bright state (*on* state). The measurement time for each mirror position ranged from 30 s to 3 min, ensuring that the QD spent enough time in the bright state. Figure 2a shows a typical period during which the intensity switches on and off. The intensity level, I_{max}, is indicated by the red line in Figure 2a, corresponding to the most common occurrence of the bright state intensity. A single exponential function fitting was used to extract the lifetime for the emission around I_{max} ($\pm\sqrt{I_{max}}$). The lifetime is plotted as a function of the distance for a single QD (QD1, batch No.: QD@618nm) in Figure 2b and another QD (QD2, batch No.: QD@639nm) in Figure 2c. The measurement was repeated three times for each QD to ensure that the distance-dependent lifetime variation was reproducible.

Since the 49-μm-diameter microsphere is much larger than both the QD size and the distance between the QD and the surface of the micro-mirror, the reflective gold layer coating on the microsphere can be approximated as a plane mirror. The relationship between the PL lifetime and separation is given by [6, 7]

$$\frac{1}{\tau} = \frac{1}{\tau_0}(1-\eta) + \frac{1}{\tau_0}\eta[(1-x)\mathrm{V(d)} + x\mathrm{H(d)}]\,. \quad (1)$$

Here τ is the PL lifetime at a certain separation, τ_0 is the lifetime in the bulk dielectric, η is the quantum yield, H and V are the distance-dependent normalized rates for horizontal and vertical dipoles, respectively, and x is the portion of the horizontal dipole. As shown by the second term on the right side of Equation (1), the mirror only changes the radiative

rate of the exciton; the intrinsic non-radiative rate in the first term cannot be changed by the optical environment. Thus, the lifetime variation is due entirely to the radiative part, and the variation in the amplitude of lifetime is determined by the QY—the ratio of the radiative decay rate to the total decay rate.

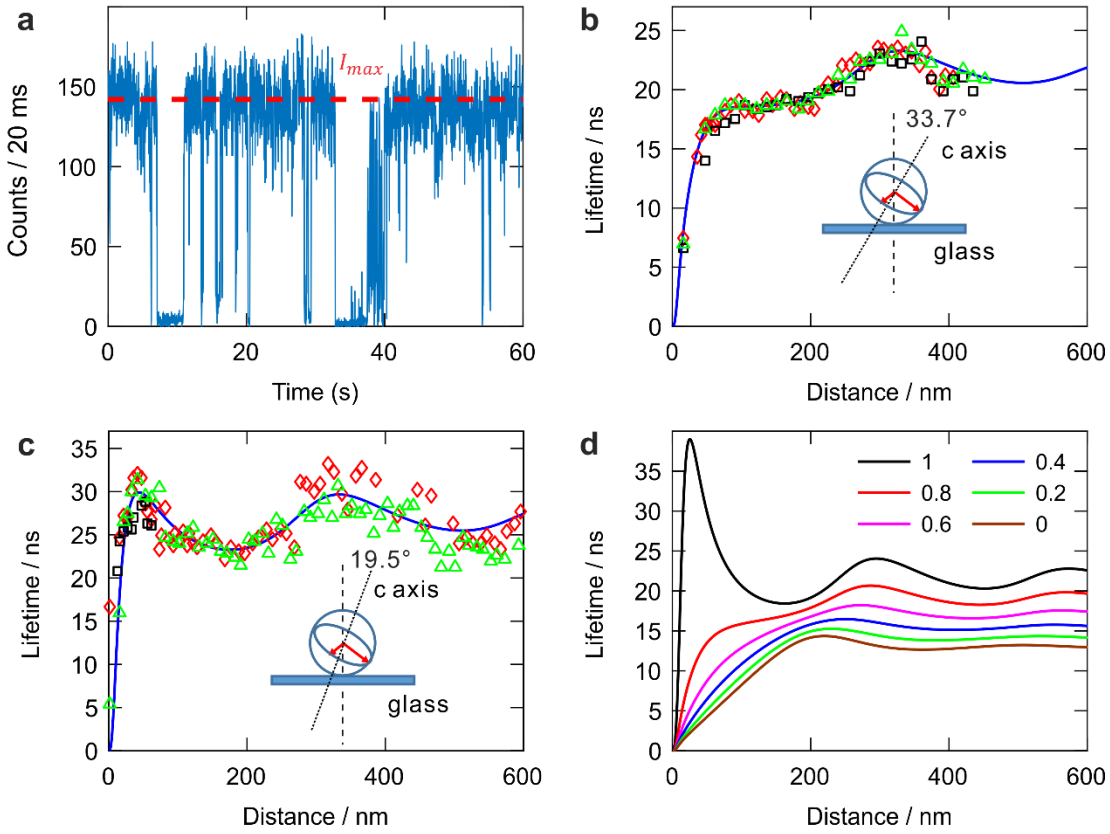

Figure 2 (a) PL intensity trace from a single QD at a certain distance from the micro-mirror. The intensity level of the bright state is selected for lifetime analysis (labeled by the red dashed line). (b) The lifetime of a single QD (QD1, batch No.: QD@618nm) as a function of the distance to the mirror. The measurement was repeated three times, corresponding to the black squares, red diamonds and green triangles. The distance-lifetime curve can be fitted to Equation (1) (blue solid line). The inset indicates the orientation of QD1 relative to the surface. The two degenerate dipoles (red arrows) are

located in the c plane. (c) Same as (b) but for another single QD (QD2, batch No.: QD@639nm). (d) Theoretical lifetime of a dipole emitter on glass as a function of the distance between the emitter and the mirror for different ratios of the vertical dipole to the horizontal dipole. The QY is 1, and wavelength is 545 nm. From the top to the bottom, the fractional contributions due to the horizontal dipole are 1, 0.8, 0.6, 0.2, and 0, respectively.

From the fitting, we can determine not only the QY but also the relative orientation of the excited state dipole moment. For QD1 in Figure 2b, the QY of the bright state is 0.90 ± 0.08, which is close to a unity QY. In Figure 2c, the bright state QY of the other QD (QD2) in Figure 2c is 0.97 ± 0.09, which is also around 1. Figure 2d shows a group of calculated distance-lifetime curves for different ratios of the horizontal dipole to the vertical dipole. As the dipole orientation shifts from vertical to horizontal, a sharp lifetime peak appears for distances shorter than 100 nm. The existence of a sharp lifetime peak for QD2 (Figure 2c) implies a larger contribution to the emission from the horizontal dipole in QD2 compared to QD1, which exhibits only a shoulder. In the case of CdSe, there is a twofold degenerate dipole perpendicular to the c-axis.[37, 38] From the optimal fit for the dipole ratio, we can determine the orientation of the QD relative to the surface plane of the glass substrate. The insets in Figure 2b and 2c illustrate the relative orientations of the two QDs, with the c-axis of QD2 aligned more vertically than that of QD1.

The effect of mirror on blinking, excitation rate and detection efficiency

In Figure 3, the blinking behaviours of a single QD (QD@618nm) are presented for two mirror distances. In Figure 3a, when the micro-mirror is fully retracted from the surface

(d = ∞), the PL intensity of the QD is high; when the mirror contacts the PMMA surface (d = 0) and its distance to the centre of the QD is less than 20 nm (the thickness of the PMMA film is about 10nm), both the PL intensity and the blinking rate are reduced. Figure 3b shows the dependence of the PL intensity on the excitation power. At the same time, the lifetime of the exciton decreases from 26.0 ns at d = ∞ to 7.0 ns at d = 0. In order to establish histograms of the *on* and *off* times, the emission is divided into *on* and *off* sections by setting the threshold level at half of the highest intensity. In Figure 3c and 3d, the distributions of *off* and *on* durations, $p_{off}(t)$ and $p_{on}(t)$, are fitted to a power-law function and a truncated power-law function, respectively:

$$p_{off}(t) \propto t^{-\alpha_{off}} \text{ for } off \text{ times; (2)}$$

$$p_{on}(t) \propto t^{-\alpha_{on}} e^{-\frac{t}{\tau_c}} \text{ for } on \text{ times. (3)}$$

In spite of the change in blinking rate in Figure 3a, the power-law distributions of *on* and *off* states, specifically, the exponents, α_{on} and α_{off}, do not change much (see Figure 3c, 3d and 3e). However, it is evident from the data in Figure 3f that both the excitation power and the mirror position affect the inverse of the truncation time for the *on* times.

According to the charging model for QD blinking, the inverse truncation time, $1/\tau_c$, characterizes the ionization rate. Under a higher excitation power, more excitons are created per unit time, and the QD is more likely to be ionized within a unit time. The dependence of the ionization rate on the excitation power is related to the mechanisms of ionization: direct (or thermal) ionization and Auger ionization.[21] Here we used a pulsed

laser to excite the QDs. The probability of direct creation of n excitons per pulse, $f(n)$, is governed by the Poisson distribution according to

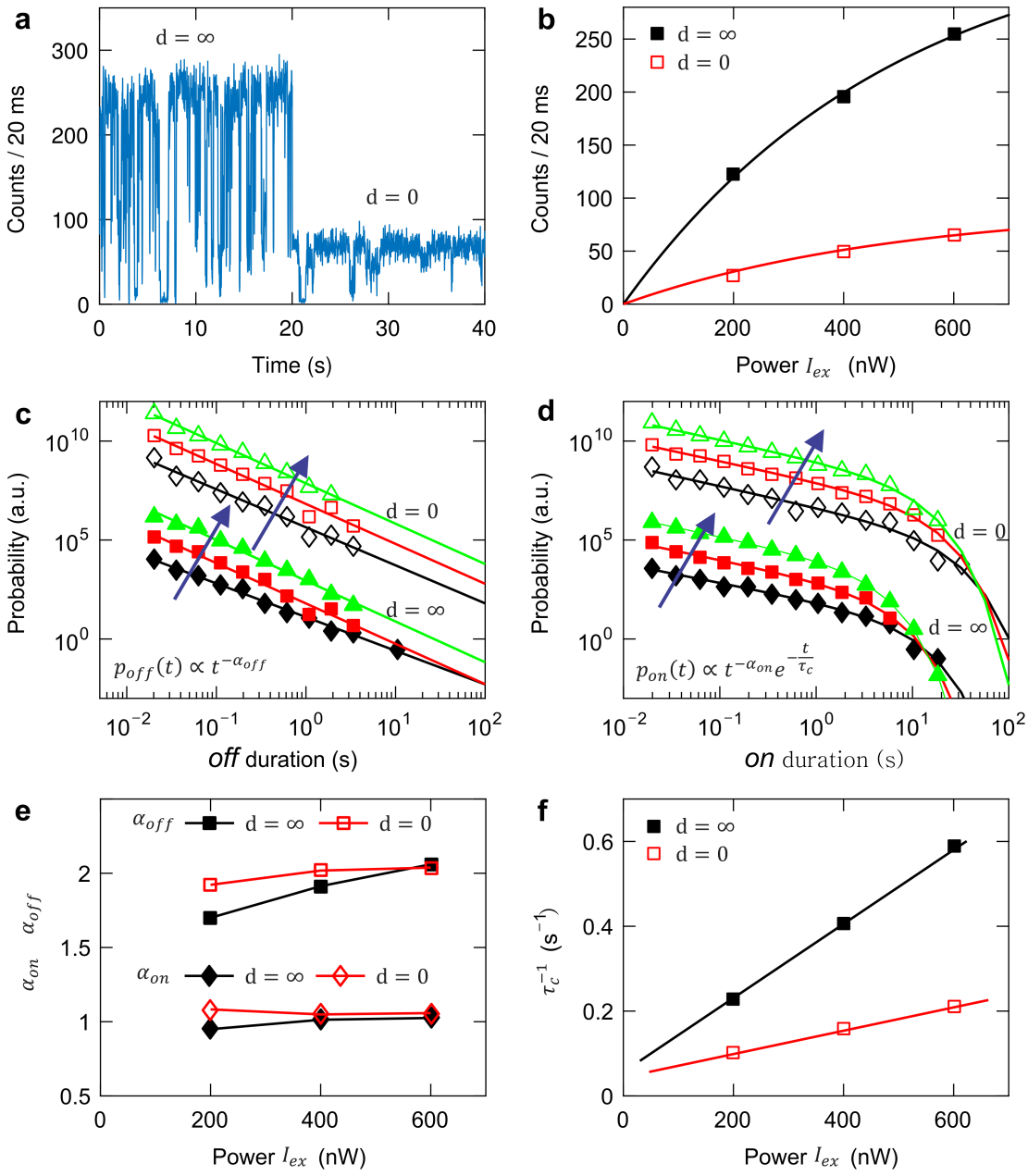

Figure 3 **(a)** PL intensity trace of a single QD (QD@618nm) far away from (d = ∞) and close to (d = 0) a micro-mirror. **(b)** Bright state intensity of the single QD close to (red open squares) and far from (black solid squares) the micro-mirror as a function of excitation power (200 nW, 400 nW and 600 nW). The solid lines indicate the nonlinear

dependence of the emission intensity on the excitation power. **(c)** The distributions of *off* state duration when the single QD is far from ($d = \infty$) and close to ($d = 0$) the micro-mirror. Blue arrows indicate the direction of increasing excitation power. Close to the micro-mirror: black open diamonds (200 nW), red open squares (400 nW) and green open triangles (600 nW). Far from the micro-mirror: black solid diamonds (200 nW), red solid squares (400 nW) and green solid triangles (600 nW). The *off* state duration distributions are fitted to a power-law function. **(d)** Same as (c) but for the *on* state duration. The solid line is the truncated power law fit. **(e)** Power-law exponents as a function of the excitation power. Red open diamonds (α_{on}, close to the micro-mirror), red open squares (α_{off}, close to the micro-mirror), black solid diamonds (α_{on}, far from the micro-mirror), black solid squares (α_{off}, far from the micro-mirror). **(f)** The inverse of the truncation times of *on* state duration as a function of excitation power when the single QD is close to (black solid squares) and far from (red open squares) the micro-mirror.

$$f(n) = \frac{N^n}{n!} e^{-N}, \quad N = \beta I_{ex}, (4)$$

where N is the average excitation rate—the average number of excitons per pulse, which is proportional to the excitation power I_{ex} with a coefficient β. If the ionization is due to direct or thermally-assisted tunneling of one excited state charge carrier, then the ionization rate is proportional to the probability of single exciton generation per pulse γ_{1x}. Under conditions of low excitation, γ_{1x} the ionization rate therefore depends linearly on the excitation power:

$$\gamma_{1x} = \sum_{n=1}^{\infty} f(n) = 1 - f(0)$$

$$= 1 - e^{-N} \approx N \propto I_{ex} \text{ for } N \to 0\,. \quad (5)$$

Note that a single exciton can be generated *via* direct excitation by laser or *via* fast Auger relaxation from a multiexciton state. Similarly, under low excitation conditions, biexciton Auger ionization results in a quadratic relationship[39] as:

$$\gamma_{2x} = \sum_{n=2}^{\infty} f(n) = 1 - f(0) - f(1)$$

$$= 1 - e^{-N} - N\,e^{-N} \approx 0.5N^2 \propto {I_{ex}}^2 \text{ for N} \to 0\,. \quad (6)$$

The current literature on the dependence of the ionization rate on the excitation power shows little consensus. Both linear[40-42] and quadratic[39, 43-45] dependences have been reported. In some cases, the ionization rate is even reported to be independent[46] of the excitation power, or exponentially dependent.[41] Figure 3f shows a linear dependence of the ionization rate on the excitation power, which does not support pure Auger ionization. However, we cannot conclude that pure single exciton ionization is occurring from the linear dependence, either, because the excitation rate is not low here. Instead, the QD is under a medium or high excitation condition (N$\sim$1 or N $>$ 1). This can be inferred from the nonlinear increase in the bright state intensity with excitation power shown in Figure 3b. Under medium or high excitation conditions, the generation rates of both single excitons and biexcitons are significant. However, the possibility of direct biexciton ionization is low due to its fast decay rate. So the direct ionization pathway should be from single excitons. Then, the ionization rate from the single exciton state should follow $1 - e^{-\beta I_{ex}}$, and should not depend linearly on the excitation power. Recently, a similar linear relation has also been found even when the average excitation rate is larger than 1.[40]

Because the generation rate of hot excitons is proportional to the excitation power, it was proposed[40] that the charging events are due to hot carrier[47] ionization. Hot carriers have enough energy to overcome any activation barrier and hence to reach surface traps. Hot carrier ionization is also supported by the observed effects of wavelength-dependent excitation.[40, 48] However, biexciton Auger recombination also produces hot carriers especially at high excitation powers. Thus, if hot carriers from excited hot excitons are the origin of ionization, then Auger ionization cannot be excluded. In summary, none of the above ionization mechanisms can explain the ionization process independently; the charging events are possibly due to several competing ionization mechanisms: band-edge carrier ionization, hot carrier ionization and biexciton Auger ionization.

Since a low excitation rate leads to a low ionization rate, the lower ionization rate at $d = 0$ may be due to the decreased excitation field induced by the mirror contacting the surface. However, we will show below that the average excitation rate remains the same for the two mirror positions, $d = 0$ and $d = \infty$. Figure 4a shows the excitation-power dependence of the bright state emission intensity for $d = 0$ and $d = \infty$. As the excitation power increases, both PL intensities become saturated. The measured PL intensity I of a single QD is the product of the average excitation rate N, quantum yield η, detection efficiency η_d, and the pulse repetition rate f as:

$$I = N\eta\eta_d f = \sum_{n=1}^{\infty} \gamma_{nx}\eta_{nx}\eta_d f. \quad (7)$$

In the above equation, we consider the contribution from n excitons with the probability γ_{nx} and QY η_{nx}. Due to the low QY for multiexciton generation ($n \geq 2$), the PL intensity arises mainly from single exciton recombination. So Equation (7) is reduced to

$$I = \gamma_{1x}\eta_{1x}\eta_d f\ . \quad (8)$$

When the average excitation rate N is high, the probability of single exciton generation per pulse γ_{1x} tends to 1 as

$$\gamma_{1x} = 1 - e^{-N} \overset{N\gg1}{\longrightarrow} 1.$$

Then the ratio of the unsaturated PL intensity I_{low} to the saturated PL intensity I_{sat} can be used to evaluate the "unsaturated probability" of single exciton generation per pulse $\gamma_{1x\ low}$ according to[24]

$$\frac{I_{low}}{I_{sat}} = \frac{\gamma_{1x\ low}\eta_{1x}\eta_d f}{1 \times \eta_{1x}\eta_d f} = \gamma_{1x\ low}. \quad (9)$$

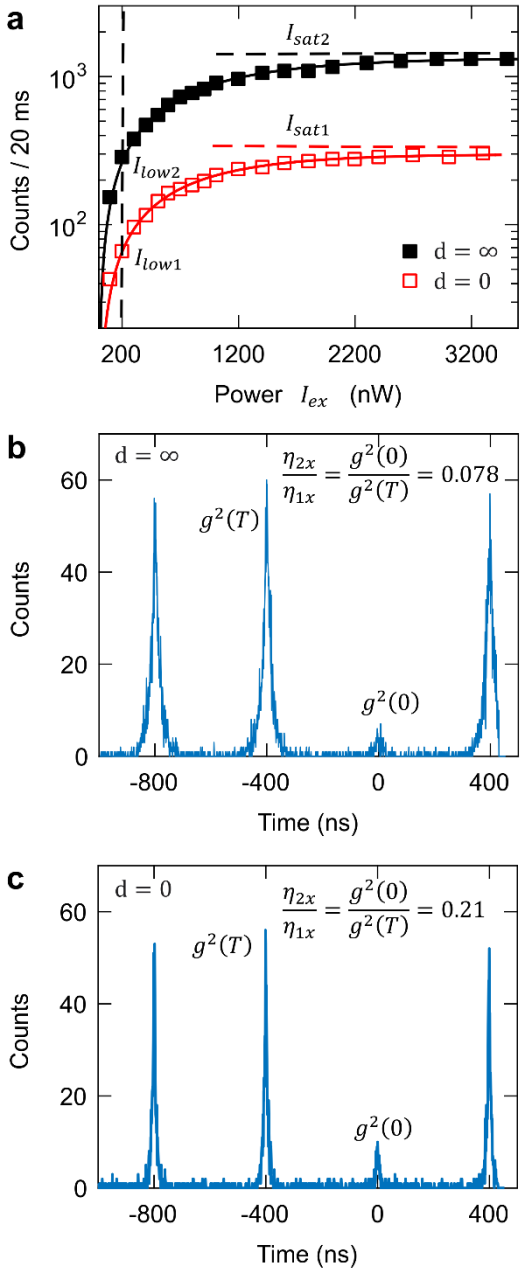

Figure 4 (a) Excitation-power dependence of the PL of a single QD (QD@618nm) with two positions of the mirror, d = ∞ (black solid squares) and d = 0 (red open squares). The solid lines are the fits to Equation (10) with biexciton QYs 0.078 for d = ∞ and 0.21 for d = 0, respectively. The laser repetition rate is 5 MHz, and the excitation power is 200 nW. (b) The g^2 measurement for the QD when d = ∞. (c) The g^2 measurement for the QD when d = 0. For g^2 measurements, the laser repetition rate is 2.5 MHz, and the excitation power is 100 nW.

We compare the unsaturated probability of single exciton generation per pulse $\gamma_{1x\,low}$ between $\mathrm{d} = 0$ and $\mathrm{d} = \infty$ at the same excitation power. We find that the ratio is unity:

$$\frac{\gamma_{1x\,low}\,(\mathrm{d} = 0)}{\gamma_{1x\,low}\,(\mathrm{d} = \infty)} = \frac{\frac{I_{low1}}{I_{sat1}}}{\frac{I_{low2}}{I_{sat2}}} \approx 1.0\,,$$

where I_{sat1} and I_{sat2} are the saturated PL intensities at high excitation conditions for $\mathrm{d} = 0$ and $\mathrm{d} = \infty$, respectively, while I_{low1} and I_{low2} are the unsaturated PL intensities at the same low excitation power (200 nW) for $\mathrm{d} = 0$ and $\mathrm{d} = \infty$, respectively. We have also measured other single QDs and found that the ratio between $\gamma_{1x\,low}$ is around 1. This means that the average excitation rate N in the vicinity of the mirror equals that far away from the mirror.

In Equation (8), we have ignored the biexciton by assuming that it has zero QY. But the QY of the biexciton is not exactly zero. Second-order PL intensity correlation measurements collected at $\mathrm{d} = \infty$ and $\mathrm{d} = 0$, are shown in Figure 4b and 4c, respectively. Under low excitation conditions (100 nW, 2.5 MHz pulsed laser), the ratio of the center peak area to side peak area is the QY ratio of biexciton to single exciton, $\frac{\eta_{2x}}{\eta_{1x}}$.[49] From $\frac{\eta_{2x}}{\eta_{1x}} = 0.078$ for $\mathrm{d} = \infty$ and $\frac{\eta_{2x}}{\eta_{1x}} = 0.21$ for $\mathrm{d} = 0$, we infer that the QY of the biexcitons is nonzero. So the PL intensity is due not only to single exciton recombination but also partially to biexcitons:

$$I = \eta_d f \eta_{1x}\left[1 - e^{-N} + \frac{\eta_{2x}}{\eta_{1x}}(1 - e^{-N} - Ne^{-N})\right],$$

$$N = \beta I_{ex}. \quad (10)$$

Using $\frac{\eta_{2x}}{\eta_{1x}} = 0.078$ for $\mathrm{d} = \infty$ and $\frac{\eta_{2x}}{\eta_{1x}} = 0.21$ for $\mathrm{d} = 0$, we can fit the excitation-power dependence of the PL intensity in Figure 4a. It is also found that

$$\frac{\beta(\mathrm{d} = 0)}{\beta(\mathrm{d} = \infty)} \approx 1.0 \,.$$

Hence, we can conclude that the mirror does not change the excitation rate when it lands on the surface. It is reasonable that there is no strong excitation field enhancement by the gold film. Firstly, the laser excitation wavelength is 466 nm at which wavelength the plasmonic effect is weak.[29] Secondly, even though the mirror is in contact with the surface, there is still a large gap between the QD and the mirror and any near-field plasmonic effect is further weakened. Thirdly, the excitation field enhancement is weak because the gold film is both thick and smooth.

Since we exclude an increased excitation rate, the only reason for the decrease in $1/\tau_c$ at $\mathrm{d} = 0$ in Figure 3f must be the shortened lifetime of the excitons induced by the mirror. The ionization rate from a single band-edge exciton is given by

$$\mathrm{k}_{ionization} = f\gamma_{1x}\frac{k_t}{k_t + k} \approx f\gamma_{1x}k_t\tau \,, (11)$$

where k_t is the trapping rate for an exciton, and k is the recombination rate. Considering the fact that the recombination rate is much faster than the trapping rate, the ionization rate $\mathrm{k}_{ionization}$ must be proportional to the lifetime of excitons. When the exciton lifetime is shortened by proximity to the mirror, the probability of ionization is reduced. A lower ionization rate can also be inferred from the Auger ionization mechanism. With the enhancement of the biexciton QY by the mirror, hot carrier generation *via* Auger recombination is suppressed. Hence, the ionization rate is reduced when the QD is close to

the mirror. Irrespective of the ionization mechanism, it is evident that the blinking can be suppressed by accelerating the radiative recombination.

In addition to determining both the QY and the excitation rate, we can also estimate the detection efficiency. The intrinsic Auger decay rate $k_{nx\,A}$ for n excitons cannot be changed by the mirror, but the radiative decay rate $k_{nx\,r}$ can be enhanced. Here we define the QY as

$$\eta_{nx} = \frac{k_{nx\,r}}{k_{nx\,r} + k_{nx\,A}} . (12)$$

The radiative decay rate refers to the total non-intrinsic decay rate including energy transfer between the QD and the mirror. This radiative emission can be divided into two parts: one can be detected ($k_{nx\,r}^{detected}$), and the other cannot be detected ($k_{nx\,r}^{nondetected}$). The radiative decay rate (total non-intrinsic decay rate) is defined as

$$k_{nx\,r} = k_{nx\,r}^{detected} + k_{nx\,r}^{nondetected} . (13)$$

So the detection efficiency η_d is defined as

$$\eta_d = \frac{k_{nx\,r}^{detected}}{k_{nx\,r}^{detected} + k_{nx\,r}^{nondetected}} . (14)$$

$k_{nx\,r}^{detected}$ and $k_{nx\,r}^{nondetected}$ scale equally with the exciton number n. Therefore, the detection efficiency η_d remains the same for excitons and biexcitons. Now we can estimate the detection efficiency from the saturation PL intensity from Figure 4a. Since the QY of the bright state is close to 1 for QD@618 nm, the detection efficiency can be determined from

$$I_{sat} = \gamma_{1x}\eta_{1x}\eta_d f = 1 \times 1 \times \eta_d f ,$$

$$\eta_d = I_{sat}/f . (15)$$

The detection efficiencies are 0.3% and 1.3% for $\mathrm{d} = 0$ and $\mathrm{d} = \infty$, respectively. When the QD is close to the mirror, the detection efficiency is reduced mainly due to the energy transfer from the QD to the mirror.

The mirror effect on biexciton QYs

The QY enhancement was investigated for a single QD (QD@618 nm) in Figure 5. Figure 5a plots the PL time decays of the bright state for $\mathrm{d} = \infty$ and $\mathrm{d} = 0$, respectively. Considering the unity QY of the bright state for QD@618nm, the lifetime of bright-state emission corresponds to the radiative lifetime of a single exciton. The ratio of the radiative decay rates of the single exciton at both separations is

$$\frac{k_{1x\,r}(\mathrm{d}=0)}{k_{1x\,r}(\mathrm{d}=\infty)} = \frac{\frac{1}{\tau_{1x\,r}(\mathrm{d}=0)}}{\frac{1}{\tau_{1x\,r}(\mathrm{d}=\infty)}} = \frac{1/(6.0\ \mathrm{ns})}{1/(21.5\ \mathrm{ns})} \approx 3.6\,.$$

Figure 5b indicates that the biexciton QYs are 0.32 at $\mathrm{d} = 0$ and 0.12 at $\mathrm{d} = \infty$, respectively. The biexciton QY at $\mathrm{d} = \infty$, 0.12, is in agreement with the literature.[50, 51] Both are independent of excitation power under low excitation conditions, in agreement with the previous report.[52] Assuming a constant Auger decay rate, the ratio of the biexciton radiative decay rate at $\mathrm{d} = 0$ to that at $\mathrm{d} = \infty$ is

$$\frac{k_{2x\,r}(\mathrm{d}=0)}{k_{2x\,r}(\mathrm{d}=\infty)} = \frac{\frac{\eta_{2x}}{1-\eta_{2x}}(\mathrm{d}=0)}{\frac{\eta_{2x}}{1-\eta_{2x}}(\mathrm{d}=\infty)} \approx 3.5\,.$$

The enhancements (3.6-fold and 3.5-fold) in both radiative decay rates are the same for exciton and biexciton because both decay rates are proportional to the increased LDOS. By assuming $k_{2x\,r} = 4k_{1x\,r}$, the Auger decay rate can be estimated from η_{2x}:

$$k_{2x\,A}(d = 0) = 1.41\ \mathrm{ns}^{-1}$$

$$\approx k_{2x\,A}(d = \infty) = 1.36\ \mathrm{ns}^{-1}.$$

This confirms that the mirror does not affect the Auger decay rate.

We have also calculated the g^2 counts per unit time. In principle, the g^2 rate, $\langle g^2 \rangle_t$, is a quadratic function of the excitation power, I_{ex}^2, as has been reported for non-blinking QDs.[52] As indicated in Figure 5c, however, the exponent here is close to 1. This can be attributed to the excitation-power dependent blinking. While the average *off* period is insensitive to the power, an increase in the excitation power leads to a decrease in the average *on* period. Assuming that the fraction of g^2 counts due to *on* periods is proportional to I_{ex}^{-q}, the exponent of $\langle g^2 \rangle_t$ becomes 2-q:

$$\langle g^2 \rangle_t \propto I_{ex}^m \propto I_{ex}^2 \cdot I_{ex}^{-q} = I_{ex}^{2-q}\,. (16)$$

Since the blinking rate is suppressed in the proximity of the mirror, the exponent, $m \approx 1.26$ at $\mathrm{d} = \infty$ is slightly larger than $m \approx 1.10$ at $\mathrm{d} = 0$.

In conclusion, we have measured the bright state QY, QD orientation, the excitation rate and the detection efficiency for single QDs. The bright states have QYs close to 100% for these single QDs. The LDOS and the excitation power do not significantly affect the *off*-time statistics, while the power-law exponents of both the *on*- and *off*-duration

distributions are independent of the position of the micro-mirror. However, because the micro-mirror shortens the lifetime of the exciton, the ionization rate is reduced.

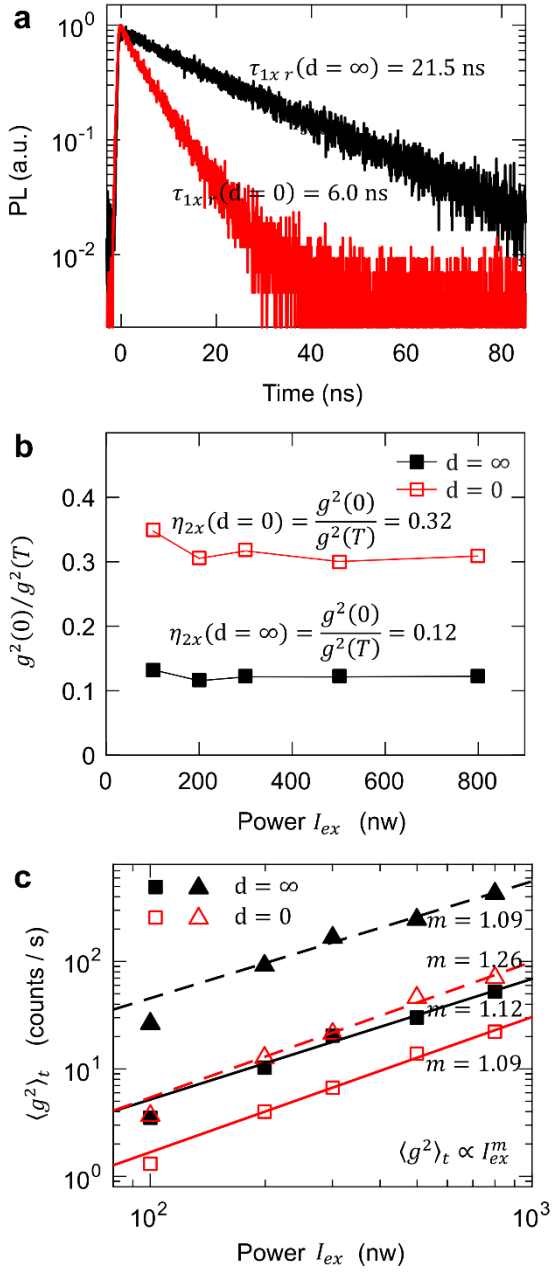

Figure 5 (a) PL time decays for a single QD with two positions of the mirror, d=∞ (black) and d=0 (red). (b) Excitation-power dependence of $g^2(0)/g^2(T)$ for the single QD with two positions of the mirror, d = ∞ (black solid squares) and d = 0 (red open squares). (c) Excitation-power dependence of g^2 rate for the single QD with two positions of the mirror, d = ∞ (solid symbols) and d = 0 (open symbols). Both central peaks $g^2(0)$

(triangles) and side peaks $g^2(T)$ (squares) are included. The laser repetition rate is 2.5 MHz, and the excitation power is 100 nW.

ASSOCIATED CONTENT

Supporting Information. Details on CdSe/$Cd_xZn_{1-x}S$ QD synthesis and QD measurements.

AUTHOR INFORMATION

Corresponding Author

Email: mulvaney@unimelb.edu.au

ACKNOWLEDGEMENTS

P.M. thanks the ARC for support through grants DP130102134 and CE170100026. G.Y. thanks the University of Melbourne for MIFR and MIEA scholarships. D.E.G. thanks the ARC for funding through a Future Fellowship (FT140100514).

REFERENCES

(1) Brouwer, A. M. *Pure Appl. Chem.* **2011,** 83, 2213-2228.

(2) Lodahl, P.; Mahmoodian, S.; Stobbe, S. *Rev. Mod. Phys.* **2015,** 87, 347-400.

(3) Würth, C.; Grabolle, M.; Pauli, J.; Spieles, M.; Resch-Genger, U. *Nat. Protocols* **2013,** 8, 1535-1550.

(4) Purcell, E. *Phys. Rev.* **1946,** 69, 681.

(5) Drexhage, K. H. *Progress in optics* **1974,** 12, 163-232.

(6) Novotny, L.; Hecht, B., *Principles of Nano-Optics*. Cambridge University Press: New York, 2006.

(7) Chance, R.; Prock, A.; Silbey, R. *Adv. Chem. Phys.* **1978,** 37, 65.

(8) Barnes, W. L. *J. Mod. Opt.* **1998,** 45, 661-699.

(9) Snoeks, E.; Lagendijk, A.; Polman, A. *Phys. Rev. Lett.* **1995,** 74, 2459-2462.

(10) Kwadrin, A.; Koenderink, A. F. *J. Phys. Chem. C* **2012,** 116, 16666-16673.

(11) Danz, N.; Heber, J.; Bräuer, A.; Kowarschik, R. *Phys. Rev. A* **2002,** 66, 063809.

(12) Chizhik, A. I.; Gregor, I.; Ernst, B.; Enderlein, J. *Chemphyschem* **2013,** 14, 505-513.

(13) Leistikow, M. D.; Johansen, J.; Kettelarij, A. J.; Lodahl, P.; Vos, W. L. *Phys. Rev. B* **2009,** 79, 045301.

(14) Lunnemann, P.; Rabouw, F. T.; van Dijk-Moes, R. J.; Pietra, F.; Vanmaekelbergh, D.; Koenderink, A. F. *ACS Nano* **2013,** 7, 5984-5992.

(15) Walters, R.; Kalkman, J.; Polman, A.; Atwater, H.; de Dood, M. *Phys. Rev. B* **2006,** 73, 132302.

(16) Frimmer, M.; Mohtashami, A.; Femius Koenderink, A. *Appl. Phys. Lett.* **2013,** 102, 121105.

(17) Buchler, B. C.; Kalkbrenner, T.; Hettich, C.; Sandoghdar, V. *Phys. Rev. Lett.* **2005,** 95, 063003.

(18) Chizhik, A. I.; Chizhik, A. M.; Khoptyar, D.; Bar, S.; Meixner, A. J.; Enderlein, J. *Nano Lett.* **2011,** 11, 1700-1703.

(19) Chizhik, A. I.; Gregor, I.; Enderlein, J. *Nano Lett.* **2013,** 13, 1348-1351.

(20) Nirmal, M.; Dabbousi, B. O.; Bawendi, M. G.; Macklin, J. *Nature* **1996,** 383, 802.

(21) Efros, A. L.; Rosen, M. *Phys. Rev. Lett.* **1997,** 78, 1110.

(22) Zhang, K.; Chang, H.; Fu, A.; Alivisatos, A. P.; Yang, H. *Nano Lett.* **2006,** 6, 843-847.

(23) Frantsuzov, P.; Volkán-Kacsó, S.; Jankó, B. *Phys. Rev. Lett.* **2009,** 103, 207402.

(24) Spinicelli, P.; Buil, S.; Quélin, X.; Mahler, B.; Dubertret, B.; Hermier, J. P. *Phys. Rev. Lett.* **2009,** 102, 136801.

(25) Brokmann, X.; Coolen, L.; Dahan, M.; Hermier, J. *Phys. Rev. Lett.* **2004,** 93, 107403.

(26) Gómez, D. E.; van Embden, J.; Jasieniak, J.; Smith, T. A.; Mulvaney, P. *Small* **2006,** 2, 204-208.

(27) Shimizu, K.; Woo, W.; Fisher, B.; Eisler, H.; Bawendi, M. *Phys. Rev. Lett.* **2002,** 89, 117401.

(28) Ito, Y.; Matsuda, K.; Kanemitsu, Y. *Phys. Rev. B* **2007,** 75, 033309.

(29) Canneson, D.; Mallek-Zouari, I.; Buil, S.; Quélin, X.; Javaux, C.; Mahler, B.; Dubertret, B.; Hermier, J. P. *Phys. Rev. B* **2011,** 84, 245423.

(30) Bharadwaj, P.; Novotny, L. *Nano Lett.* **2011,** 11, 2137-2141.

(31) Kolchin, P.; Pholchai, N.; Mikkelsen, M. H.; Oh, J.; Ota, S.; Islam, M. S.; Yin, X.; Zhang, X. *Nano Lett.* **2015,** 15, 464-468.

(32) Ma, X.; Tan, H.; Kipp, T.; Mews, A. *Nano Lett.* **2010,** 10, 4166-4174.

(33) Ratchford, D.; Shafiei, F.; Kim, S.; Gray, S. K.; Li, X. *Nano Lett.* **2011,** 11, 1049-1054.

(34) Shafran, E.; Mangum, B. D.; Gerton, J. M. *Phys. Rev. Lett.* **2011,** 107, 037403.

(35) Tuna, Y.; Kim, J. T.; Liu, H. W.; Sandoghdar, V. *ACS Nano* **2017,** 11, 7674-7678.

(36) Boldt, K.; Kirkwood, N.; Beane, G. A.; Mulvaney, P. *Chem. Mater.* **2013,** 25, 4731-4738.

(37) Chung, I.; Shimizu, K. T.; Bawendi, M. G. *Proc. Natl. Acad. Sci. U.S.A.* **2003,** 100, 405-408.

(38) Efros, A. L.; Rosen, M.; Kuno, M.; Nirmal, M.; Norris, D. J.; Bawendi, M. *Phys. Rev. B* **1996,** 54, 4843.

(39) Peterson, J. J.; Nesbitt, D. J. *Nano Lett.* **2008,** 9, 338-345.

(40) Meng, R.; Qin, H.; Niu, Y.; Fang, W.; Yang, S.; Lin, X.; Cao, H.; Ma, J.; Lin, W.; Tong, L.; Peng, X. *J. Phys. Chem. Lett.* **2016,** 7, 5176-5182.

(41) Stefani, F. D.; Knoll, W.; Kreiter, M.; Zhong, X.; Han, M. Y. *Phys. Rev. B* **2005,** 72, 125304.

(42) Banin, U.; Bruchez, M.; Alivisatos, A. P.; Ha, T.; Weiss, S.; Chemla, D. S. *J. Chem. Phys.* **1999,** 110, 1195-1201.

(43) Eremchev, I. Y.; Osad'ko, I. S.; Naumov, A. V. *J. Phys. Chem. C* **2016,** 120, 22004-22011.

(44) Cordones, A. A.; Bixby, T. J.; Leone, S. R. *J. Phys. Chem. C* **2011,** 115, 6341-6349.

(45) Bruhn, B.; Qejvanaj, F.; Sychugov, I.; Linnros, J. *J. Phys. Chem. C* **2014,** 118, 2202-2208.

(46) Knappenberger, K. L.; Wong, D. B.; Romanyuk, Y. E.; Leone, S. R. *Nano Lett.* **2007,** 7, 3869-3874.

(47) Galland, C.; Ghosh, Y.; Steinbruck, A.; Sykora, M.; Hollingsworth, J. A.; Klimov, V. I.; Htoon, H. *Nature* **2011,** 479, 203-207.

(48) Gómez, D. E.; van Embden, J.; Mulvaney, P.; Fernee, M. J.; Rubinsztein-Dunlop, H. *ACS Nano* **2009,** 3, 2281-2287.

(49) Nair, G.; Zhao, J.; Bawendi, M. G. *Nano Lett.* **2011,** 11, 1136-1140.

(50) Fisher, B.; Caruge, J. M.; Zehnder, D.; Bawendi, M. *Phys. Rev. Lett.* **2005,** 94, 087403.

(51) Zhao, J.; Nair, G.; Fisher, B. R.; Bawendi, M. G. *Phys. Rev. Lett.* **2010,** 104, 157403.

(52) Park, Y. S.; Malko, A. V.; Vela, J.; Chen, Y.; Ghosh, Y.; Garcia-Santamaria, F.; Hollingsworth, J. A.; Klimov, V. I.; Htoon, H. *Phys. Rev. Lett.* **2011,** 106, 187401.

FOR TOC ONLY